Charge-induced effects on the structure and properties of silane and disilane derivatives

D. Balamurugan* and R. Prasad
Department of Physics, Indian Institute of Technology, Kanpur 208016, India
(Received 16 August 2005; revised manuscript received 2 May 2006; published 16 June 2006)

Using *ab-initio* electronic structure methods, we have investigated the ground state structures and properties of neutral and charged $SiH_m(m=1-4)$ and $Si_2H_n(n=1-6)$ clusters that are produced in the plasma enhanced chemical vapor deposition process used in the preparation of hydrogenated amorphous silicon (*a*-Si:H). Our results show that charging a neutral cluster distorts it and the distortion mainly occurs through the orientation of a Si-H bond. We attribute structural changes in the charged clusters to electrostatic repulsion between the bonded and nonbonded electrons. We find that in addition to the usual Si-H bond, hydrogen atoms form Si-H-H and Si-H-Si bonds in some clusters. The vibrations of Si-H, Si-Si, Si-H-Si bond stretching modes show that the frequencies are shifted significantly upon charging. The frequency shifts in the charged clusters are consistent with their bond length variations. We discuss the fragmentation pathways of silane into binary products and the role of fragmented silane radicals in the cluster formation and *a*-Si:H film deposition process.

DOI: 10.1103/PhysRevB.73.235415 PACS number(s): 73.22.−f, 31.15.Ar, 36.40.Wa, 36.40.Mr

I. INTRODUCTION

Silane (SiH_4) is used in the plasma enhanced chemical vapor deposition (PECVD) process to produce hydrogenated amorphous silicon (*a*-Si:H) that has potential applications in solar cells and flat panel devices. Before *a*-Si:H film deposition takes place, the gaseous silane molecules are decomposed either by using an electric field[1] or by thermal energy.[2] The decomposed species live for a short time in a plasma environment and contribute to *a*-Si:H film growth. In the plasma, the decomposed species exist also in charged states. Experimental studies[2–11] have shown the presence of various neutral and charged species in the plasma such as Si, SiH_3, and Si_2H_6, and SiH_3^+, $Si_2H_5^+$, and Si_xH^+ $(x=4-10)$. Also, the experimental investigations[1,3,4,12–14] show that the decomposed species have a great influence on the properties of *a*-Si:H films. Therefore, investigating the structure and properties of neutral and charged silane and disilane derivatives can help in gaining a better understanding of *a*-Si:H film growth in the PECVD process. With this motivation we have carried out *ab-initio* electronic structure calculations to study (1) the ground state structure, (2) vibrational frequencies, (3) fragmentation, and (4) clustering process of neutral and charged SiH_m $(m=1-4)$ and Si_2H_n $(n=1-6)$ clusters.

In the recent past, several electronic structure calculations have been presented on neutral and charged silane and disilane derivatives at various levels of accuracy.[15–20] The ground and excited states of SiH have been investigated using the multireference configuration interaction approach.[15] Using a configuration interaction and coupled cluster method with single and double excitations, a detailed vibrational analysis on SiH_3^- has been performed.[16] Coupled cluster calculations have been carried out to study the ground state structures and vibrational properties of SiH_n $(n=2-4)$ clusters.[17] Grev and Schaefer[18] applied coupled cluster method to identify the local minima of Si_2H_2. Gupte and Prasad[19] reported ground state structures and vibrational frequencies of Si_nH_m $(n=1,2$ and $m=1-6)$ clusters using nonorthogonal tight binding molecular dynamics. Recently, the potential energy surface of Si_2H^- has been explored[20] using coupled cluster and configuration interaction methods. However, *ab-initio* calculations on neutral and charged silane and disilane derivatives using the same methodology are still lacking. We haveperformed density functional theory calculations to understand the charge induced effects on the structure and properties of silane and disilane derivatives.

The fragmentation and the clustering reactions of silane derivatives in the PECVD process are not yet well understood. Phenomenological model calculations have been carried out to understand the formation of various clusters during silane discharge and their role on film deposition process.[6,21] Using semiempirical method the collisions between Si^+ and H_2 over a range of collision energies have been studied.[22] Sosa and Lee[23] performed density functional theory calculations to study the insertion reactions of SiH_2, SiHF, and SiF_2 into H_2 and found that fluorine substitution increases the reaction barrier heights. In a series of theoretical investigations, Raghavachari[24–27] showed that the sequential clustering reactions of silane with the Si^+, SiH^+, SiH_2^+, and SiH_3^+ end with different products such as $Si_2H_4^+$, $Si_2H_5^+$, $Si_3H_3^+$, $Si_3H_5^+$, $Si_4H_7^+$, $Si_5H_{10}^+$, and $Si_5H_{11}^+$. We have also investigated the fragmentation of silane and the role of the fragmented radicals in the beginning steps of the clustering process.

Our *ab-initio* calculations on neutral and charged SiH_m $(m=1-4)$ and Si_2H_n $(n=1-6)$ clusters show several interesting findings about their ground state structures and properties. We find that in addition to the usual Si-H bond, hydrogen atoms in some clusters form Si-H-H and Si-H-Si bonds. Charging the cluster affects the Si-H bond orientations and Si-H, Si-H-Si, and Si-Si bond lengths. We explain the bond orientations and bond length variations of the charged clusters using molecular orbital, charge density, and population analysis.

We have performed a vibrational analysis of the neutral and charged clusters and find that the frequencies of stretching modes of Si-H, Si-Si, and H-Si-H bonds shift considerably upon charging. These frequency shifts are consistent with the bond length variations of the charged clusters. The fragmentation studies on neutral and charged silane show

that the major radicals formed are SiH_2, SiH_2^+, SiH_3^+, and SiH_3^-. These radicals undergo further clustering processes, which lead to disilane derivatives. We also discuss the possible role of these radicals in *a*-Si:H film deposition process.

The plan of the paper is as follows. In Sec. II we give computational details of the present work. In Sec. III we present and discuss in detail the ground state geometries of neutral and charged silane and disilane derivatives. A vibrational analysis of these clusters is discussed in Sec. IV. In Sec. V we discuss the fragmentation of silane and the formation of bigger hydrogenated silicon clusters. Finally, in Sec. VI we give our conclusions.

II. COMPUTATIONAL DETAILS

We have used the Car-Parrinello molecular dynamics(CPMD)[28,29] and GAUSSIAN98[30] package for our study. Using the CPMD method[31,32] with simulated annealing optimization, we have obtained the ground state structures of the neutral clusters. The pseudopotentials for silicon and hydrogen have been generated using the Bachelet, Hamann, and Schlüter technique.[33] The local density approximation (LDA) of the density functional theory has been used with the Ceperley-Alder[34] exchange-correlation energy functional parametrized by Perdew and Zunger.[35] The wave functions were expanded in a plane wave basis with 12 Rydberg energy cutoff and $\mathbf{k}=0$ point was used for Brillouin zone sampling. During simulation, the volume of the system was kept constant, and to avoid an interaction between the clusters, a big fcc supercell with a side length of 35 a.u. was used. To perform simulated annealing, the system was taken to high temperatures (1200 K in the steps of 300 K), equilibrated for a long time (about 16 000 steps) and then slowly cooled down (in the steps of 50 K) to 300 K. Below this temperature, the steepest descent optimization was found to be more efficient to obtain the ground state geometry. The desired temperature was achieved by rescaling atomic velocities, and the atoms were moved according to the velocity Verlet algorithm[36] with a time step of 5 a.u. The fictitious mass of the electron was taken to be 200 a.u. Our SiH_n ($n=2-4$) and Si_2H_2 ground state structures obtained using the CPMD method are in good agreement with those found earlier[17,18] using *ab-initio* quantum chemical calculations.

For obtaining the ground state structures of the charged clusters,[37] we have used the GAUSSIAN98 package. We have taken the structures of neutral clusters obtained from the CPMD calculations and reoptimized the neutral and charged clusters using the GAUSSIAN98 package by Berny's optimization technique.[38] The geometry optimization has been done with Becke's three parameter hybrid functional (B3LYP) for an exchange-correlation functional and employing a 6-311g** basis set.[30,39] The vibrational frequencies of the neutral and charged clusters are calculated with the same functional and basis set. We see from Table I that the ionization potentials (IP) of the clusters obtained from Gaussian calculations are in good agreement with the experimental values.[40–42] The IP values of Si and Si_2 have been calculated with various multiplicities to take account of the orbital degeneracy. We find that the ground state of Si, Si^+, Si_2, and Si_2^+ have multiplicities 3, 2, 3, and 4, respectively. The IP values of Si and Si_2 reported in Table I have been obtained using the ground state multiplicities. Our calculated umbrella mode frequency 894 cm^{-1} of SiH_3^- is in excellent agreement with the experimental value[43]of 880 cm^{-1}.

TABLE I. Our calculated ionization potentials (IP) of Si_mH_n clusters using the GAUSSIAN98 package. The experimental values (a) (Ref. 40), (b) (Ref. 41), and (c) (Ref. 42) are given in the last column.

	GAUSSIAN98 IP (eV)	Experiment IP (eV)
Si	8.1	8.2(a)
SiH	8.0	7.9(a)
SiH_2	9.0	9(a)
SiH_3	8.1	8(a)
SiH_4	11.0	11(a), 12.4(b)
Si_2	7.8	7.7(c)
Si_2H	8.4	7.9(c)
Si_2H_2	8.0	7.7(c)
Si_2H_3	7.8	7.8(c)
Si_2H_4	7.9	7.6(c)
Si_2H_5	7.7	7.7(c)
Si_2H_6	9.6	7.9(c)

III. GROUND STATE STRUCTURES

A. Charge induced structural modifications

In this section we discuss the charge induced effects on the structures of SiH_m ($m=1-4$) and Si_2H_n ($n=1-6$) clusters. In Figs. 1 and 2 we have shown the ground state structures of neutral and charged silane and disilane derivatives obtained using the GAUSSIAN98 package employing B3LYP/6-311G**. From Fig. 1 we see that the structure of SiH_2 is asymmetrical top whose bond angle opens up when positively charged and does not change much when negatively charged. The structure of SiH_3 is pyramidal, which becomes planar when positively charged and Si-H bonds further bend when negatively charged.

The ground state structure of SiH_4 has tetrahedral symmetry. This symmetry is destroyed upon charging[41,44,45] and we see in Fig. 1 that SiH_4^+ and SiH_4^- have very different structures. This symmetry breaking has been attributed to the Jahn-Teller effect.[45–48] The structure of SiH_4^+ obtained by our calculation is in agreement with the structure obtained by earlier calculations.[49–53] Our ground state of SiH_5^+ is in good agreement with the result obtained by Boo and Lee.[54] The structure of SiH_5^+ is more like a complex of SiH_3^+ and H_2 and that of SiH_5^- is more like a complex of SiH_4^- and H.

Interestingly, two H atoms in SiH_4^+ and SiH_5^+ are overcoordinated and form a Si-H-H bond. This Si-H-H bond is formed between three atoms by two electrons and is an example of the multicenter bond.[55] A similar type of the three center-two electron bond, C-H-H bond, has been observed[55,56] in CH_5^+. It was predicted that due to the three

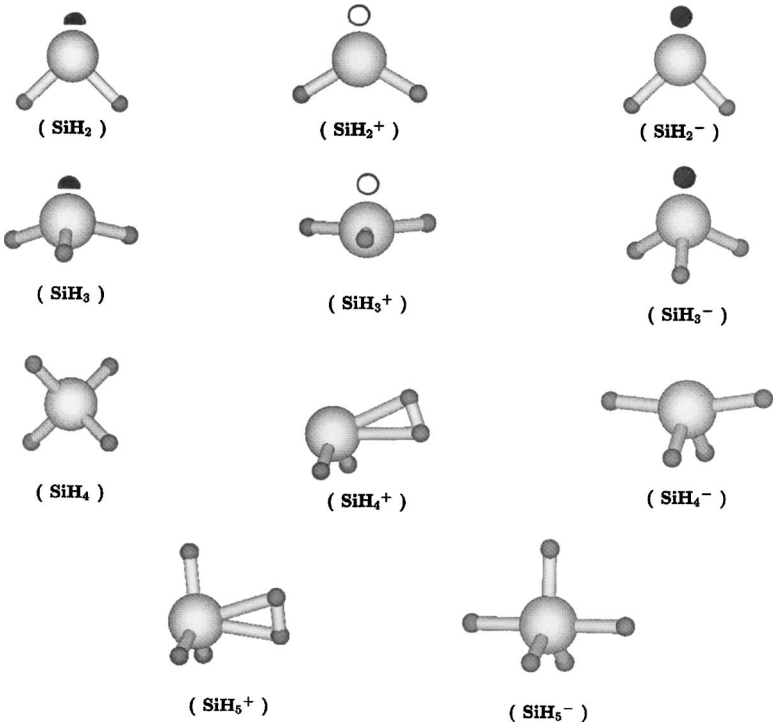

FIG. 1. The ground state structures of neutral and charged $SiH_m(m=2-4)$ clusters. Also, the structures of SiH_5^+ and SiH_5^- clusters are shown. All the structures have been obtained using the GAUSSIAN98 program employing B3LYP/6 -311G**. The gray ball represents the Si atom and the small black ball represents, the H atom. Note that Si and H atoms are connected by bonds. In addition to the position of atoms, the nonbonded electron density distribution is also shown schematically by unconnected half, open and filled circles for neutral, positive, and negative clusters, respectively. The unconnected open and filled circles, respectively, represent the decrease and increase in the nonbonded electron density.

center-two electron bond, SiH_5^+ and CH_5^+ have functional behavior,[54–56] that is, these molecules do not have a definite structure and bonding arrangement, which makes it difficult to characterize them using spectroscopic techniques. These results show that charging clusters not only changes the structure but also can give rise to the formation of unusual bonds.

The overcoordination of the H atom has also been seen in neutral clusters such as Si_2H, Si_2H_2, and Si_2H_3. We see from Fig. 2 that the hydrogen atom is overcoordinated in these clusters by connecting both silicon atoms and forms a Si-H -Si bridge bond. Note that the Si-H-Si bridge bond is a multicentered bond and is different from the Si-H bond, which is a two-centered bond.[32] The Si-H-Si bridge bonded frame of the clusters does not change when the clusters are charged. In the case of negatively charged Si_2H_2, hydrogen atoms are slightly pushed away from each other without changing each Si-H-Si frame.

Now we discuss the charge induced effects on the structure of disilane derivatives. From Fig. 2 we see that Si-H bonds of Si_2H_3 are tilted away from the Si-Si bond when positively charged and toward the Si-Si bond when negatively charged. Si_2H_4 is nearly planar and results in a perfectly planar structure when positively charged. On the other hand, Si-H bonds of Si_2H_4 tilt significantly out of plane when negatively charged. Si_2H_5 consist of SiH_3 and SiH_2 units connected by a Si-Si bond. We see from the figure that H atoms of SiH_2 unit in $Si_2H_5^+$ move slightly upward while those in $Si_2H_5^-$ are further pushed down. From the figure we see thatSi_2H_6 consist of two SiH_3 units connected by the Si -Si bond. Upon charging there is no significant change in the overall structure, but each SiH_3 units of $Si_2H_6^+$ and $Si_2H_6^-$ distort as those of SiH_3^+ and SiH_3^- clusters. The ground states of neutral and charged silane and disilane derivatives show that the structural modifications occur mainly through the bending of Si-H bonds.

The charge induced structural distortions of silane and disilane derivatives can be understood from the nature of valance electron density distribution. First, we discuss the nature of valance electron distribution and its influence on charged SiH_2 structure. Then, using the same arguments we explain the structural modifications of other charged clusters. The valence electron density distribution of neutral and charged SiH_2 are shown in Fig. 3. From the figure we see that the electron density of SiH_2 is highly localized near H atoms and also on top of the silicon atom. We call the electron density between Si and H as bonded while on the top of Si as nonbonded. This nonbonded electron distribution is in some sense, similar to the Lewis dot[57] of unpaired electrons. The density of bonded electrons is highly localized near H atoms due to the fact that hydrogen is more electronegative[58] and withdraws electron from a silicon atom. We see from the figure that the nonbonded electron density of SiH_2, on the top Si atom, decreases when positively charged and increases when negatively charged. Thus, in Fig. 1 for SiH_2, the nonbonded electron density is schematically represented by a half filled circle on Si. For SiH_2^+ it is shown by an open circle, indicating the decrease in the nonbonded electron density, while for SiH_2^- it is shown by a filled circle, indicating the increase in the nonbonded electron density.

Now we discuss how the structural modifications of charged SiH_2 can be understood in terms of the bonded and nonbonded electron density. Since the ground state of SiH_2 is not a linear geometry, the nonbonded electron density would exert a downward force on the bonded electron density. Since the nonbonded electron density of SiH_2^+ is lower than that of neutral SiH_2, its downward push on H atoms of SiH_2^+ is also lower than that of neutral SiH_2, which results in the opening of the H-Si-H bond angle. From this argument one would expect that SiH_2^{++} should have a further opening in the bond angle. Indeed, we find that the optimization on SiH_2^{++}

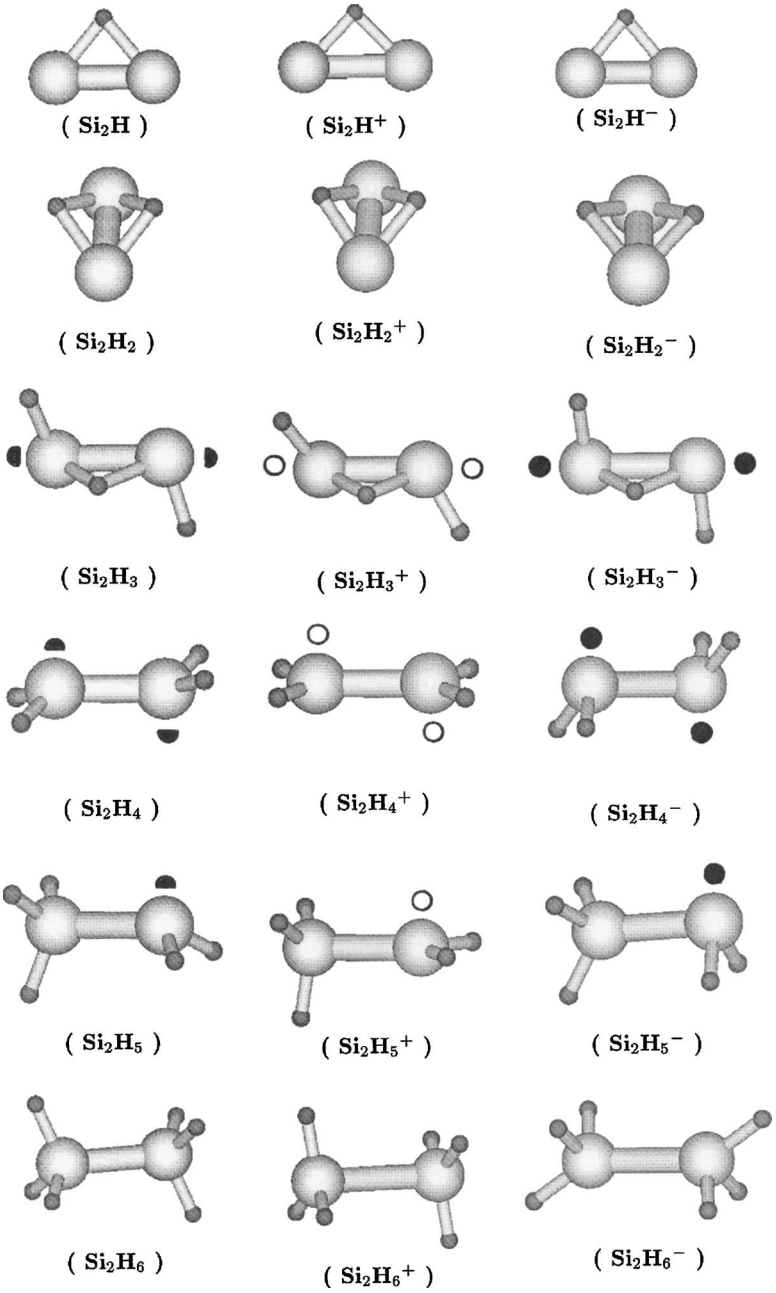

FIG. 2. The same as in Fig. 1, except for neutral and charged Si_2H_n ($n=1-6$) clusters.

results in an almost linear geometry with a larger bond angle. In contrast, in SiH_2^- there is increment in the nonbonded electron density on top of the silicon atom. Thus, one would expect that the bond angle should get smaller than that of the neutral cluster due to the excess push on H atoms. But the reduction of a H-Si-H angle is opposed by the increased H-H repulsion. The H-Hrepulsion in SiH_2^- increases because charges on H increase when SiH_2 is negatively charged.[59]

The structural modifications of other charged clusters can be explained using the same arguments given in the last paragraph. To understand the nature of valence electron distribution, we have done a charge density analysis of all these

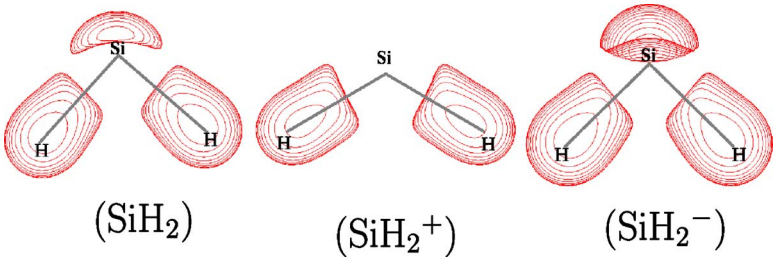

FIG. 3. (Color online) The valence electron density distribution of neutral and charged SiH_2 clusters. The isocontour value of 0.07 is chosen to show clearly the density distribution variation between the neutral and charged SiH_2. The locations of Si and H atoms are also indicated.

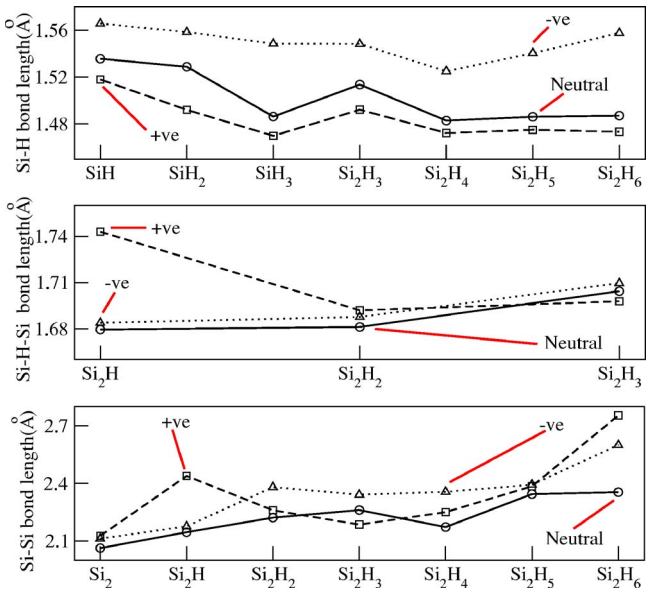

FIG. 4. (Color online) (a) Si-H, (b) Si-H-Si, and (c) Si-Si bond lengths (Å) of neutral and charged Si_nH_m ($n=1$ or 2, $m=0-6$) clusters as a function of the cluster size. Note that for the Si-H-Si bond, it is the Si-H distance that is plotted. The circles connected by a thick line represents the bond lengths of neutral clusters, the square connected by a broken line for positively charged, and triangles connected by a dotted line for negatively charged clusters.

clusters. We find that the nonbonded electron density distribution decreases when positively charged and increases when negatively charged. From the charge density analysis we have also located the nonbonded electron density in these clusters. As in the case of neutral and charged SiH_2 clusters, the nonbonded electron density is schematically represented by half, open, and filled circles for the neutral, positive, and negative clusters in Figs. 1 and 2. From this schematic representation, it is easy to understand the structural modifications in the charged clusters. Hydrogen atoms bonded to Si are attracted to the nearby open circle while they are repelled away from the nearby filled circle. The attraction of H to an open circle and the repulsion of H to a filled circle are due to the electrostatic interaction, as explained in the case of charged SiH_2 clusters.

B. Charge induced bond length variations

We find that charging the clusters not only changes Si-H bond orientations but also Si-H, Si-H-Si, and Si-Si bond lengths. In Figs. 4(a)–4(c), we have shown Si-H, Si-H-Si, and Si-Si bond lengths of the neutral and charged clusters as a function of cluster size. We see from the figure that the Si-H bond length of a positively charged cluster is shorter than that of the corresponding neutral cluster while it is longer for the negatively charged cluster. On the other hand, Si-H-Si and Si-Si bond lengths of both a positive as well as a negative charged cluster are longer than that of the neutral cluster. However, $Si_2H_3^+$ is an exception where Si-Si and Si -H-Si bond lengths are shorter than those of the neutral cluster. From Fig. 4(c), we see that the Si-Si bond length of a neutralSi_2H_n cluster increases as a function of H and reaches a maximum for Si_2H_6, but the bond length of Si_2H_4 is shorter than that of its neighboring Si_2H_3 and Si_2H_5 clusters.

To understand the Si-Si and Si-H bond length variations of charged silane and disilane derivatives, we first consider the bond length variations of Si_2 and SiH dimers. Si_2 has a bond length of 2.144 Å, the bond expands in both the positive as well as the negative charged state to 2.308 and 2.453 Å respectively. On the other hand, depending on the charged state, the bond length of the SiH dimer decreases or increases. The SiH dimer has a bond length of 1.536 Å, which shortens to 1.518 Å when positively charged and expands to 1.566 Å when negatively charged. The different trends seen in the bond lengths of charged Si_2 and SiH dimers can be understood, with the results obtained from a population analysis. The population analysis on charged dimers is done by keeping the bond distance the same as those of neutral dimers. The population analysis on Si_2 shows that each atom of the neutral dimer has a zero charge, whereas each atom of Si_2^+ has $+0.5e$ and that of Si_2^- has $-0.5e$. The atoms of charged Si_2 are equally charged and repel each other, which results in bond length expansion in both a positive and negative charged state. The population analysis on a neutral SiH dimer shows a net charge of $+0.35e$ on Si and $-0.35e$ on the H atom. The charge transfer from silicon to hydrogen is the indication of a polar covalent[60] bond, which is consistent, considering the fact that the electronegativity of silicon is smaller than hydrogen.[58] The population analysis on SiH^+ shows that the silicon atom in the dimer holds a charge of $+1.36e$ and hydrogen $-0.36e$. This means that the lost electron is primarily from the Si atom in the SiH dimer. Hence the positively charged silicon pulls the H atom closer and reduces the bond length. In the negative charged state, the Si atom carries a charge of $-0.68e$ and the H atom, a charge of $-0.32e$, and this shows that the extra electron is accumulated primarily on the silicon atom. This extra electron density on the Si of SiH^- repels the H atom and results in the bond length expansion. Our population analysis on a neutral and charged SiH dimer shows that the Si atom holds the excess charge in SiH^+ and SiH^-. This can be understood by considering the energies required to add or remove an electron from Si and H atoms. The Si atom has a smaller ionization potential (IP) than the H atom while it has larger electron affinity (EA) than the H atom.[61] Therefore adding or removing an electron from Si is easier with respect to H atom.

The general trends of Si-Si and Si-H bond length variations of charged clusters are consistent with the bond length variations of Si_2 and SiH dimers when charged. As mentioned earlier, the Si-H-Si bond expands under both charged states. In the Si-H-Si unit, two silicon atoms are also bonded, and they expand irrespective of the charged state. As a result of the Si-Si expansion, the Si-H-Si bridge bond expands under a positive as well as a negative charged state.

The shorter Si-Si bond observed in Si_2H_4 is due to the formation of a π bond between silicon atoms. The π bond has a shorter bond length when compared to a σ bond.[62] The highest occupied molecular orbital (HOMO) of Si_2H_4, Si_2H_3, and $Si_2H_3^+$ are shown in Fig. 5. From the figure we see that the HOMO of Si_2H_4 is spread above and below the line

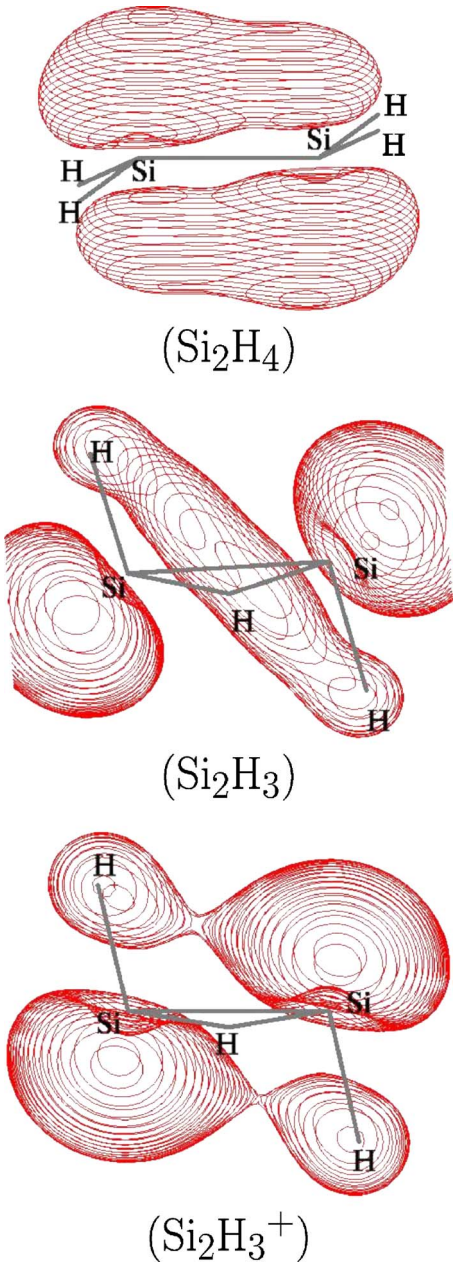

FIG. 5. (Color online) Isocontour distribution of HOMO in Si_2H_4, Si_2H_3, and $Si_2H_3^+$.

connecting the two Si atoms. This indicates that the HOMO of Si_2H_4 is formed due to the side overlap between valance p orbitals of silicon atoms, which is a characteristic of π bonding.[62] $Si_2H_3^+$ has shorter Si-Si and Si-H-Si bonds compared to the corresponding neutral cluster. From Fig. 5 we see that the HOMO of $Si_2H_3^+$ is slightly spread above and below the Si-Si bond while such a spread is absent in neutral Si_2H_3. This means that the HOMO of $Si_2H_3^+$ has gained a slightly π character compared to that of neutral Si_2H_3, and hence the Si-Si bond is shorter than that of the neutral cluster. Due to the reduction in the Si-Si bond length, the Si-H -Si bond length of $Si_2H_3^+$ is also reduced from that of the neutral cluster.

TABLE II. The calculated vibrational frequencies ν (cm^{-1}) and force constants k (mDyne/Å) of neutral and charged $SiH_m(m=1-4)$ and also charged SiH_5 clusters using the B3LYP functional employing 6-311g** basis set. Important modes such as stretch, breathing, etc., have been identified.

		SiH		SiH^+		SiH^-	
	Mode	ν	k	ν	k	ν	k
1	Si-H stretch	2013	2.49	2137	2.81	1827	2.0512
		SiH_2		SiH_2^+		SiH_2^-	
1	H-Si-H breathing	1024	0.64	907	0.51	967	0.58
2	Si-H stretch	2036	2.55	2140	2.76	1843	2.09
3	Si-H stretch	2038	2.55	2225	3.09	1852	2.10
		SiH_3		SiH_3^+		SiH_3^-	
1	Umbrella	760	0.37	839	1.11	894	0.51
2		936	0.54	940	1.11	972	0.51
3		936	0.54	940	1.05	972	0.57
4	Si-H stretch	2192	2.87	2274	3.07	1885	2.19
5	Si-H stretch	2233	3.10	2356	3.47	1885	2.19
6	Si-H stretch	2233	3.10	2357	3.47	1899	2.19
		SiH_4		SiH_4^+		SiH_4^-	
1		922	0.55	244	0.04	712	0.04
2		922	0.55	622	0.26	796	0.39
3		922	0.55	675	0.28	814	0.42
4		980	0.57	751	0.34	992	0.63
5		980	0.57	874	0.48	1038	0.64
6		2235	2.97	1043	0.65	1341	1.11
7		2243	3.12	2216	2.96	1448	1.25
8		2244	3.12	2292	3.29	2007	2.47
9		2244	3.12	3794	8.55	2008	2.46
		SiH_5^+		SiH_5^-			
1		63	0.00	513	0.16		
2		636	0.25	516	0.16		
3		656	0.26	992	0.66		
4		745	0.37	1041	0.71		
5		869	0.46	1041	0.71		
6		923	0.53	1204	0.86		
7		926	0.53	1205	0.86		
8		1046	0.65	1354	1.09		
9		2289	3.12	1506	1.38		
10		2350	3.45	1924	2.29		
11		2360	3.48	1924	2.29		
12		3955	9.29	1955	2.27		

IV. VIBRATIONAL ANALYSIS

In this section we discuss the charge induced effects on vibrational frequencies of the clusters. Also, we identify the modes corresponding to the internal rotation of subunits in the clusters. The vibrational frequencies and force constants of silane and disilane derivatives are given in Tables II and III. Our calculated vibrational frequencies 922, 980, 2235,

TABLE III. The calculated vibrational frequencies ν (cm^{-1}) and force constants k (mDyne/Å) of neutral and charged Si_2H_n(n =1–4) clusters using the B3LYP functional employing a 6-311g** basis set. Si-H-Si (∥) mode corresponds to the motion of the H atom parallel to the Si-Si bond of the cluster and Si-H-Si (⊥) corresponds to the motion of the H atom perpendicular to the Si-Si bond.

		Si_2		Si_2^+		Si_2^-	
	Mode	ν	k	ν	k	ν	k
1	Si-Si stretch	600	5.94	546	4.92	586	5.65
		Si_2H		Si_2H^+		Si_2H^-	
1	Si-Si stretch	543	4.02	407	2.22	556	4.29
2	Si-H-Si (∥)	1108	0.76	890	0.49	1104	0.75
3	Si-H-Si (⊥)	1565	1.49	1384	1.17	1479	1.33
		Si_2H_2		$Si_2H_2^+$		$Si_2H_2^-$	
1	Si-Si stretch	522	1.93	395	1.00	346	0.40
2		963	0.59	993	0.63	782	0.44
3	Si-H-Si (∥)	1083	0.72	1054	0.68	948	0.55
4	Si-H-Si (∥)	1175	0.86	1171	0.86	954	0.56
5	Si-H-Si (⊥)	1534	1.43	1546	1.45	1418	1.22
6	Si-H-Si (⊥)	1616	1.57	1626	1.59	1550	1.44
		Si_2H_3		$Si_2H_3^+$		$Si_2H_3^-$	
1		358.	0.07	198	0.02	496	0.15
2	Si-Si stretch	446.	1.57	442	0.38	415	1.53
3		647	0.26	575	0.27	688	0.29
4		739.	0.35	637	0.27	788	0.39
5		741.	0.34	772	0.38	802	0.41
6	Si-H-Si (∥)	1090	0.71	1082	0.70	1118	0.75
7	Si-H-Si (⊥)	1497.	1.37	1606	1.57	1375	1.16
8	Si-H stretch	2082	2.66	2192	2.96	1888	2.19
9	Si-H stretch	2089.	2.68	2199	2.97	1908	2.24
		Si_2H_4		$Si_2H_4^+$		$Si_2H_4^-$	
1		323	0.09	336	0.08	198	0.02
2		348	0.07	345	0.07	360	0.08
3		448	0.13	370	0.08	458	0.12
4		525	0.16	524	0.17	676	0.31
5	Si-Si stretch	563	0.78	505	1.30	390	0.95
6		616	0.27	607	0.26	677	0.30
7		919	0.53	853	0.45	936	0.54
8		956	0.58	942	0.56	943	0.55
9	Si-H stretch	2224	3.00	2279	3.14	1998	2.43
10	Si-H stretch	2228	3.01	2281	3.14	2000	2.47
11	Si-H stretch	2245	3.13	2326	3.38	2009	2.46
12	Si-H stretch	2257	3.17	2334	3.40	2019	2.52
		Si_2H_5		$Si_2H_5^+$		$Si_2H_5^-$	
1		128	0.01	40	0.00	175	0.02
2		390	0.09	340	0.11	366	0.70
3		406	0.12	362	0.08	390	0.09
4	Si-Si stretch	424	0.41	397	0.21	398	0.10
5		597	0.25	608	0.26	676	0.32
6		637	0.28	676	0.32	696	0.32
7		876	0.49	817	0.43	923	0.55
8		936	0.55	910	0.50	939	0.54
9		949	0.56	921	0.52	970	0.58
10		951	0.55	976	0.60	974	0.58
11	Si-H stretch	2188	2.90	2235	3.01	1932	2.30
12	Si-H stretch	2199	2.95	2252	3.08	1935	2.28
13	Si-H stretch	2214	3.04	2280	3.19	2040	2.56
14	Si-H stretch	2223	3.01	2291	3.26	2072	2.65
15	Si-H stretch	2231	3.09	2304	3.30	2083	2.63
		Si_2H_6		$Si_2H_6^+$		$Si_2H_6^-$	
1		131	0.01	105	0.01	162	0.02
2		380	0.09	208	0.22	211	0.23
3		380	0.09	265	0.04	250	0.04
4	Si-Si stretch	423	0.75	267	0.04	285	0.05
5		636	0.29	328	0.07	498	0.18
6		636	0.29	328	0.07	562	0.22
7		855	0.47	723	0.34	855	0.47
8		928	0.56	789	0.40	884	0.49
9		945	0.54	918	0.52	932	0.53
10		945	0.54	918	0.52	938	0.53
11		959	0.56	928	0.53	962	0.58
12		959	0.56	928	0.53	966	0.56
13	Si-H stretch	2209	2.93	2256	3.03	1765	1.91
14	Si-H stretch	2217	2.99	2258	3.03	1826	2.03
15	Si-H stretch	2218	3.02	2314	3.33	2058	2.62
16	Si-H stretch	2219	3.03	2315	3.34	2061	2.58
17	Si-H stretch	2227	3.08	2321	3.36	2069	2.60
18	Si-H stretch	2229	3.08	2322	3.36	2076	2.66

and 2244 cm^{-1} for SiH_4 are in good agreement with those of experimentally obtained values[63] of 914, 953, 2189, and 2267 cm^{-1}.

We notice from the tables that SiH_4^+, SiH_5^+, $Si_2H_3^+$, $Si_2H_4^-$, neutral and charged clusters of Si_2H_5 and Si_2H_6, have one mode with very low frequency and nearly a zero force constant. A small frequency and force constant for a mode imply that during the vibrational motion the atoms of the cluster move in a nearly constant potential energy surface. This may be an indication that the mode corresponds to either a transition state or internal rotation[45,64–66] of the cluster. We looked into the vibrational motion corresponding to low frequency modes of the clusters. We find that the low frequency modes are associated with the internal rotation of subunits about some symmetry axis of the clusters.

One vibrational frequency of SiH_3 corresponds to the umbrella mode. The umbrella mode frequency of SiH_3 is 760 cm^{-1}, which increases for both SiH_3^+ and SiH_3^- to 839 and 894 cm^{-1} respectively. The inversion barriers for SiH_3 and SiH_3^- are 0.22 and 1.24 eV, respectively. Because of the increased barrier height, the frequency of SiH_3^- is larger than that of SiH_3. Although SiH_3^+ is planar without an inversion barrier, the frequency and force constant of the umbrella mode are larger than those of the neutral and negative clus-

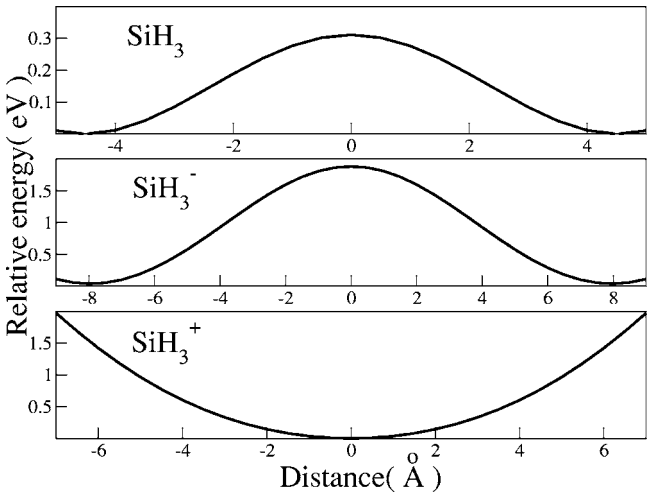

FIG. 6. The total energy of SiH_3, SiH_3^-, and SiH_3^+ as a function of the Si distance from the center of inversion. For each cluster the total energy is given with respect to its ground state energy. All these sets of calculations have been performed by varying the Si distance along the symmetry axis and freezing H atoms. Since H atoms are frozen in the present set of calculations, for each cluster the total energy at the inversion center shown in the figure is slightly overestimated in comparison with the fully geometry optimized energy referred to in the text. Note that 0.0 Å means that the Si atom is at the inversion center and the structure of the cluster is planar.

ters. This is due to the fact that the potential energy surface of SiH_3^+ about the center of inversion has a different shape from those of SiH_3 and SiH_3^-. At the inversion center, SiH_3 and SiH_3^- have barriers while SiH_3^+ has a potential energy minimum, as shown in Fig. 6.

We find that charging the cluster shifts the stretching frequency of Si-H, Si-Si, and H-Si-H bonds. From Tables II and III, we see that the trend of frequency variations in Si -H, Si-Si, and Si-H-Si stretch modes of charged clusters is opposite to the trend of their bond length variations, which is shown in Fig. 4. For example, the Si-H stretch frequency of a SiH dimer is 2013 cm^{-1}, which increases to 2137 cm^{-1} for SiH^+ and decreases to 1827 cm^{-1} for SiH^-. From Fig. 4, we see that the bond length is shorter for SiH^+ while it is longer for $SiH^-$from that of the neutral SiH dimer. Such a relationship between the Si-H bond length variation and frequency variation seen in the SiH dimer holds true for Si-H, Si-Si, and Si-H-Si bonds of all the clusters. In general, a longer bond length reduces the frequency, and vice versa. This relationship is reasonable since an expansion of the bond means that the bond gets weaker and hence the corresponding stretch mode has a lower frequency. On the other hand, shortening of the bond length means that the bond gets stronger and hence the stretch mode has a larger frequency.

V. FRAGMENTATION OF SILANE AND THE FORMATION OF BIGGER CLUSTERS

A. Fragmentation of neutral and charged silane

For the fragmentation studies, we have considered various possible fragmentation pathways of silane into binary products. Also the charged clusters are included in our investigation as they exist in a PECVD plasma. The fragmentation energy of a cluster has been calculated by taking the difference between the total energy of the reactant with those of product clusters. Among the possible fragmentation channels of neutral and charged silane, the low energy channels are

$$SiH_4 \rightarrow SiH_2 + H_2(+2.57\ \text{eV}), \quad (1)$$

$$SiH_4^+ \rightarrow SiH_2^+ + H_2(+0.60\ \text{eV}), \quad (2)$$

$$SiH_4^- \rightarrow SiH_3^- + H(+1.33\ \text{eV}), \quad (3)$$

where the number in parentheses is the fragmentation energy.

As we see from the previous reactions, the production of hydrogen in molecular form is favored in SiH_4 and SiH_4^+ while atomic hydrogen is favored in SiH_4^-. Our low energy fragmentation channel of SiH_4 agrees with the experimental study.[8] There is another process where the hydrogen atom is attached with SiH_4^+ and forms SiH_5^+, which undergoes fragmentation, as given later,

$$SiH_4^+ + H \rightarrow SiH_5^+ \rightarrow SiH_3^+ + H_2(+0.64\ \text{eV}). \quad (4)$$

This process is quite possible since a large amount of hydrogen is available in the PECVD plasma, and we see from the fragmentation energies of SiH_4^+ and SiH_5^+ that the latter is more stable to the fragmentation of H_2. We find that the energy required to break H_2 from SiH_5^- is negative and is about −0.24 eV. This indicates that SiH_5^- is highly unstable. Therefore, SiH_5^- is not considered in our fragmentation study.

It has been observed that deposition of SiH_3 on the film improves the material quality whereas the deposition of SiH and SiH_2 degrades the material quality.[1] Therefore, it is important to understand the production of SiH_3 and its role on the film deposition process. We see from Eqs. (3) and (4) that SiH_3^- and SiH_3^+ are produced in the fragmentation process after attaching an electron with a SiH_4 and the hydrogen atom with SiH_4^+. This indicates that the production of SiH_3 can be improved by controlling the electron and H content in the PECVD plasma. It is interesting to compare these processes with the experimental investigation[67] on argon/hydrogen expanding thermal plasma. The investigation suggests that a significant amount of SiH_3 is produced by electron collision and hydrogen collision process.

The structure and dipole moment of SiH_3 may play a role on improving the a:Si-H film quality. As we have mentioned, SiH_3 has low inversion barriers of 0.22 eV. This implies that SiH_3 can transform to a planar structure from its ground state pyramidal structure by crossing the barrier. The barrier crossing can easily occur in the hot plasma environment. When the cluster transforms into the planar structure, its dipole moment changes by a considerable amount. The dipole moment of pyramidal SiH_3 is 0.16D and that of planar SiH_3 is zero. Because of its zero dipole moment the planar SiH_3 does not get easily physisorbed on the film. This low physisorbtion behavior of a planar SiH_3 cluster is similar to that of CH_3 in hydrogenated amorphous carbon film deposition.[68] Since the planar SiH_3 has a low physisorbtion property, it can migrate on the surface until it gets absorbed

by a highly reactive site, which could be a dangling bond, surface void or some defect. The surface gets smoothened due to the migration of planar SiH_3, as a result the film quality improves.

B. Formation of bigger clusters

We have shown in the silane fragmentation process that the product radicals are SiH_2, SiH_2^+, SiH_3^+, and SiH_3^-. These radicals are reactive as they have unsaturated bonds and can react with silane and with each other, forming new species.[3–7,21] The new species formed in the clustering process of the radicals with silane are

$$SiH_2 + SiH_4 \rightarrow Si_2H_6(-2.29\ \text{eV}), \quad (5)$$

$$SiH_2^+ + SiH_4 \rightarrow Si_2H_6^+(-1.68\ \text{eV}), \quad (6)$$

$$SiH_3^+ + SiH_4 \rightarrow Si_2H_5^+ + H_2(-0.33\ \text{eV}), \quad (7)$$

$$SiH_3^- + SiH_4 \rightarrow Si_2H_5^- + H_2(-0.29\ \text{eV}). \quad (8)$$

As we see from the previous equations, the interaction of SiH_2 with SiH_4 resulting in Si_2H_6 is highly favored, which agrees well with the experimental results.[5,8]

The species formed by clustering of the radicals with each other are

$$SiH_2 + SiH_2 \rightarrow Si_2H_4(-2.63\ \text{eV}), \quad (9)$$

$$SiH_2 + SiH_2^+ \rightarrow Si_2H_4^+(-3.71\ \text{eV}), \quad (10)$$

$$SiH_2 + SiH_3^+ \rightarrow Si_2H_5^+(-2.90\ \text{eV}), \quad (11)$$

$$SiH_2 + SiH_3^- \rightarrow Si_2H_5^-(-2.86\ \text{eV}), \quad (12)$$

$$SiH_3^+ + SiH_3^- \rightarrow Si_2H_6(-10.00\ \text{eV}). \quad (13)$$

The number in the parentheses is the cluster formation energy for the process, which is calculated by taking the total energy difference between the product and the reactant clusters.

Except Si_2H_6 and $Si_2H_6^+$, other products formed in the previous reactions undergo further clustering processes, as they have unsaturated bonds. Since $Si_2H_6^+$ is saturated with hydrogen, it favors fragmentation. Si_2H_6 is the immediate stable cluster formed by the reaction of silane fragmented radicals. It is interesting to see that recent experimental observations[2,5,8,67] show a sufficient amount of Si_2H_6 in silane decomposed PECVD plasma.

VI. CONCLUSIONS

Using the *ab initio* electronic structure methods, we have found the ground state structures of neutral and charged silane, disilane, and their decomposed species. Interestingly, in addition to the usual Si-H bond, hydrogen forms Si-H-Si and Si-H-H bonds in some of these clusters; it forms a Si-H-Si bridge bond in Si_2H, Si_2H_2, and Si_2H_3 clusters and a three-center two electron Si-H-H bond in SiH_4^+ and SiH_5^+ clusters. We find that charging the clusters induces structural modifications that mainly occur through Si-H bond orientations. We attribute these structural modifications to the electrostatic repulsion between the nonbonded electrons and bonded electrons.

We find that the Si-H bond of a Si_mH_n cluster is shortened when positively charged and expanded when negatively charged. On the other hand, the Si-Si and Si-H-Si bonds of the cluster expand, irrespective of the charged state. The bond length variations of Si-H and Si-Si bonds in the charged clusters are similar to that of charged SiH and Si_2 dimers.

Our vibrational analysis shows that frequencies of Si-H, Si-Si, Si-H-Si stretch modes show significant changes when the clusters are charged. These frequency shifts are consistent with their bond length variations.

We have shown that the low energy pathways of fragmenting neutral and charged silane are associated with SiH_2, SiH_2^+, SiH_3^+, and SiH_3^- products. The fragmentation results indicate that the production of SiH_3 can be controlled by the electron and H content in the PECVD plasma. We speculate that the experimentally observed[1] improvement in *a*-S:H film quality by SiH_3 deposition is due to the surface migration of planar SiH_3. The investigation on the clustering process shows that Si_2H_6 is the immediate stable cluster formed by the silane decomposed radicals, which is consistent with the experimental observations[2,5,8,67]

ACKNOWLEDGMENT

It is a pleasure to thank S. C. Agarwal and M. K. Harbola for helpful discussions and comments. This work was supported by the Department of Science and Technology, New Delhi via Project No. SP/S2/M-51/96.

*Present address: Department of Chemistry, Tulane University, New Orleans, LA 70118

[1] W. M. M. Kessels, R. J. Severens, A. H. Smets, B. A. Korevaar, G. J. Adriaenssens, D. C. Schran, and M. C. M. van de Sanden, J. Appl. Phys. **89**, 2404 (2001).

[2] H. L. Duan, G. A. Zaharias, and S. F. Bent, Appl. Phys. Lett. **78**, 1784 (2001).

[3] G. Bano, P. Horvath, K. Rozsa, and A. Gallagher, J. Appl. Phys. **98**, 13304 (2005).

[4] A. Gallagher, A. A. Howling, and Ch. Hollenstein, J. Appl. Phys. **91**, 5571 (2002).

[5] P. Horvath, K. Rozsa, and A. Gallagher, J. Appl. Phys. **96**, 7660 (2004).

[6] M. A. Childs and A. Gallagher, J. Appl. Phys. **87**, 1076 (2000).

[7] J. R. Doyle, D. A. Doughty, and A. Gallagher, J. Appl. Phys. **71**, 4771 (1992).

[8] J. R. Doyle, D. A. Doughty, and A. Gallagher, J. Appl. Phys. **71**, 4727 (1992).
[9] A. Leroux, W. M. M. Kessels, D. C. Schram, and M. C. M. van de Sanden, J. Appl. Phys. **88**, 537 (2000).
[10] J. R. Doyle, D. A. Doughty, and A. Gallagher, J. Appl. Phys. **68**, 4375 (1990).
[11] D. A. Doughty and A. Gallagher, Phys. Rev. A **42**, 6166 (1990).
[12] A. von Keudell and J. R. Abelson, Phys. Rev. B **59**, 5791 (1999).
[13] B. M. Jelenkovic and A. Gallagher, J. Appl. Phys. **82**, 1546 (1997).
[14] D. M. Tanenbaum, A. L. Laracuente, and A. Gallagher, Appl. Phys. Lett. **68**, 1705 (1996).
[15] A. Kalemos, A. Mavridis, and A. Metropoulos, J. Chem. Phys. **116**, 6529 (2002).
[16] M. Shen, Y. Xie, and H. Schaefer III, J. Chem. Phys. **93**, 8098 (1990).
[17] W. D. Allen and H. F. Schaefer III, Chem. Phys. **108**, 243 (1986).
[18] R. S. Grev and H. F. Schaefer III, J. Chem. Phys. **97**, 7990 (1992).
[19] G. R. Gupte and R. Prasad, Int. J. Mod. Phys. B **12**, 1607 (1998); G. R. Gupte and R. Prasad, *ibid.* **12**, 1737 (1998).
[20] C. Pak, L. Sari, J. C. Rienstra-Kiracofe, S. S. Wesolowski, L. Horny, Y. Yamaguchi, and H. F. Schaefer III, J. Chem. Phys. **118**, 7256 (2003).
[21] A. Gallagher, Phys. Rev. E **62**, 2690 (2000).
[22] N. Chaâbane, H. Vach, and G. H. Peslherbe, J. Non-Cryst. Solids **299-302**, 42 (2002).
[23] C. Sosa and C. Lee, J. Chem. Phys. **98**, 8004 (1993).
[24] K. Raghavachari, J. Chem. Phys. **92**, 452 (1990).
[25] K. Raghavachari, J. Chem. Phys. **95**, 7373 (1991).
[26] K. Raghavachari, J. Chem. Phys. **96**, 4440 (1992).
[27] K. Raghavachari, J. Chem. Phys. **88**, 1688 (1988).
[28] R. Car and M. Parrinello, Phys. Rev. Lett. **55**, 2471 (1985).
[29] For a review, see, for example,M. Parrinello, Solid State Commun. **102**, 107 (1997); D. K. Remler and P. A. Madden, Mol. Phys. **70**, 921 (1990).
[30] GAUSSIAN98, Revision A.11.1, M. J. Frisch *et al.*, Gaussian, Inc., Pittsburgh PA, 2001.
[31] The computational procedure for our CPMD calculation on SiH_m, and Si_2H_m clusters is similar to that of our earlier CPMD calculations done on Si_m ($m=2-10$), and Si_mH ($m=1-10$) clusters (Ref. 32).
[32] D. Balamurugan and R. Prasad, Phys. Rev. B **64**, 205406 (2001).
[33] G. B. Bachelet, D. R. Hamann, and M. Schlüter, Phys. Rev. B **26**, 4199 (1982).
[34] D. M. Ceperley and B. J. Alder, Phys. Rev. Lett. **45**, 566 (1980).
[35] J. P. Perdew and A. Zunger, Phys. Rev. B **23**, 5048 (1981).
[36] See, for example, J. M. Haile, *Molecular Dynamics Simulation* (Wiley, New York, 1992).
[37] Here we would like to point out the difficulties in performing plane wave calculations for negatively charged clusters. We have performed plane wave pseudopotential calculations as implemented in the VASP package (Ref. 69) for positive, and negative charged clusters. The VASP set of calculations has been performed with ultrasoft pseudopotential (Ref. 69) using the local density approximation (LDA) (Refs. 34 and 35). We have used 150 eV Ecut for neutral, and charged clusters. Calculations on neutral as well as charged clusters have been performed using a simple cubic supercell of 20 Å length. This length is sufficiently big enough to isolate the clusters from their supercell image (Ref. 70). Moreover, VASP handles the charged systems by applying a background charge to maintain the charge neutrality, and by adding dipole, and quadrupole corrections (Refs. 71 and 72). Using the big supercell with the added corrections, we find that the VASP calculated total energies, and structures of positive clusters are good while those of negative clusters are not good. In the negatively charged clusters, the uppermost electron is highly diffusive in nature. Therefore, negative clusters require an even larger supercell. Since GAUSSIAN package calculations are performed in real space, the image problem that occurs in the supercell technique can be avoided. All the values reported for the clusters in this article have been obtained using the GAUSSIAN package.
[38] H. B. Schlegel, J. Comput. Chem. **3**, 214 (1982); H. B. Schlegel, "Geometry Optimization on Potential Energy Surfaces," in *Modern Electronic Structure Theory*, edited by D. R. Yarkony (World Scientific Publishing, Singapore, 1994).
[39] J. B. Foresman and A. Frisch, *Exploring Chemistry with Electronic Structure Methods*, 2nd ed. (Gaussian, Inc., Pittsburgh, PA, 1993).
[40] J. Berkowitz, J. P. Greene, H. Cho, and B. Ruščić, J. Chem. Phys. **86**, 1235 (1987).
[41] U. Itoh, Y. Toyashima, H. Onuki, N. Washida, and T. Ibuki, J. Chem. Phys. **85**, 4867 (1986).
[42] R. Robertson and A. Gallagher, J. Appl. Phys. **59**, 3402 (1986).
[43] M. R. Nimlos and G. B. Ellison, J. Am. Chem. Soc. **108**, 6522 (1986).
[44] The symmetry breaking of charged SiH_4 clusters and their vibrational properties have been discussed earlier (Ref. 45). For the sake of completeness we have included some results in this paper.
[45] D. Balamurugan, M. K. Harbola, and R. Prasad, Phys. Rev. A **69**, 033201 (2004).
[46] I. B. Bersuker, Chem. Rev. (Washington, D.C.) **101**, 1067 (2001).
[47] M. D. Sturge in *The Jahn-Teller Effect in Solids*, edited by F. Sietz, D. Turnbull, and H. Ehrenreich, Vol. 20 of Solid State Physics, Advances in Research, and Applications (Academic, New York, 1967), p. 91.
[48] R. Englman, *The Jahn-Teller Effect in Molecules, and Crystals* (Wiley-Interscience, New York, 1972).
[49] R. F. Frey and E. R. Davidson, J. Chem. Phys. **89**, 4227 (1988).
[50] F. D. Proft and P. Geerlings, Chem. Phys. Lett. **262**, 782 (1996).
[51] T. Kudo and S. Nagase, Chem. Phys. **122**, 233 (1988).
[52] R. Caballol, J. A. Catala, and J. M. Problet, Chem. Phys. Lett. **130**, 278 (1986).
[53] A. R. Porter, O. K. Al-Mushadani, M. D. Towler, and R. J. Needs, J. Chem. Phys. **114**, 7795 (2001).
[54] D. W. Boo and Y. T. Lee, J. Chem. Phys. **103**, 514 (1995).
[55] D. Marx and M. Parrinello, Science **284**, 59 (1999).
[56] D. Marx and A. Savin, Angew. Chem., Int. Ed. Engl. **36**, 2077 (1997).
[57] See, for example, I. N. Levine, *Quantum Chemistry* (Prentice–Hall, Englewood Cliffs, NJ, 1991), pp. 503–506.
[58] J. Robles and L. J. Bartolotti, J. Am. Chem. Soc. **106**, 3723 (1984).
[59] The population analysis gives charges on Si, and H in SiH_2^-, respectively, as $-0.48e$, and $-0.26e$ while for neutral SiH_2 the corresponding charges are $0.30e$, and $-0.15e$. The population numbers given here, and in the other parts of the text refer to the amount of charge on each atom with respect to the nuclear

charge obtained from natural population analysis using B3LYP/6-311G** calculations.

[60] A. Beiser, *Perspectives of Modern Physics* (McGraw-Hill, New York, 1985), p. 300.

[61] *CRC Handbook of Chemistry and Physics*, 85th ed., edited by D. R. Lide (CRC, Boca Raton, FL, 2004); O. A. Vydrov and G. E. Scuseria, J. Chem. Phys. **122**, 184107 (2005).

[62] J. W. Moore, C. L. Stanitski, and P. C. Jurs, *Chemistry, The Molecular Science*, 2nd ed. (Brooks/Cole-Thomson Learning, Belmont, 2005), p. 349.

[63] A. M. Coats, D. C. McKean, and D. Steele, J. Mol. Struct. **320**, 269 (1994).

[64] C. R. Quade, J. Mol. Spectrosc. **188**, 190 (1998).

[65] P. Y. Ayala and H. B. Schlegel, J. Chem. Phys. **108**, 2314 (1998).

[66] Y. Duan, R. Wang, and I. Mukhopadhyay, Chem. Phys. **280**, 119 (2002).

[67] M. C. M. van de Sanden, R. J. Serverens, W. M. M. Kessels, R. F. G. Meulenbroeks, and D. C. Schram, J. Appl. Phys. **84**, 2426 (1998).

[68] J. Perrin, M. Shiratani, P. Kae-Nune, H. Videlot, J. Jolly, and J. Guillon, J. Vac. Sci. Technol. A **16**, 278 (1998).

[69] G. Kresse and J. Furthmüller, Comput. Mater. Sci. **6**, 15 (1996); Phys. Rev. B **54**, 11169 (1996).

[70] V. Kumar and Y. Kawazoe, Phys. Rev. Lett. **90**, 055502 (2003).

[71] G. Makov and M. C. Payne, Phys. Rev. B **51**, 4014 (1995); G. Makov, R. Shah, and M. C. Payne, *ibid.* **53**, 15513 (1996).

[72] J. Neugebauer and M. Scheffler, Phys. Rev. B **46**, 16067 (1992).